Article
https://doi.org/10.31489/2025PH1/77-88
UDC 621.785

Received: 17.12.2024
Accepted: 28.01.2025

L.G. Sulyubayeva[1], D.B. Buitkenov[1], D.R. Baizhan[1],
N.E. Berdimuratov[1], N.S. Raisov[1*], A.Zh. Zhumabekov[2]

[1]*Research Center Surface Engineering and Tribology, Sarsen Amanzholov East Kazakhstan University, Ust-Kamenogorsk, Kazakhstan;*
[2]*Toraigyrov University, Pavlodar, Kazakhstan*
*(*Corresponding author's e-mail: nurmakhanbetraisov@gmail.com)*

Influence of Thermocyclic Electrolyte-Plasma Treatment on Mechanical Properties of U9 Tool Steel

The article investigates the influence of thermocyclic electrolytic-plasma treatment (EPT) on the mechanical properties of carbon steel U9 tool steel. U9 steel is often used for manufacturing tools working in conditions that do not cause edge heating: woodworking tools, assembly tools, gauges of simple shape and reduced accuracy classes. In this work, thermocyclic electrolytic-plasma treatment was used as a method of improving mechanical properties. This method combines electrochemical reactions and intensive thermal influence, which allows the formation of surface layers with improved characteristics. As a result of the treatment, U9 steel shows a clear division of the microstructure into three zones: hardened layer, transition layer and base metal. The hardened layer, located up to a depth of 400 μm, is characterized by a finely dispersed structure consisting of martensite and bainite with high hardness (1400–1600 $HV_{0.1}$). This layer provides excellent wear resistance and resistance to mechanical stress. The transition layer (400–700 μm) serves as a buffer zone, distributing stresses evenly. It is characterized by a gradual decrease in hardness (800–1200 $HV_{0.1}$) and a change in structure due to a decrease in martensite content. The base metal, deeper than 700 μm, retains the original structure with hardness 400–600 $HV_{0.1}$, which ensures its ductility and durability. The results show that thermocyclic EPT significantly improves the performance properties of U9 steel by creating a functionally gradient structure. The technology is energy efficient and can be widely used in mechanical engineering and other industries where high mechanical characteristics of materials are required.

Keywords: heat treatment, thermocyclic electrolytic-plasma treatment, electric discharge phenomena, U9 tool steel, microstructure, micro hardness

Introduction

In conditions when traditional materials in mechanical engineering and equipment manufacturing exhaust their capabilities and do not meet the growing requirements of modern technologies, the introduction of innovative approaches and technologies becomes critical. Development and application of new materials and processing methods are necessary to improve the performance, strength and durability of assemblies and mechanisms. One of the key solutions is the modernization of technological processes aimed at improving the reliability and life of parts. This includes the use of advanced methods such as chemical-thermal treatment, thermocyclic hardening, anodic-spark oxidation and electrolyte-plasma technologies [1–6].

Electrolyte-plasma treatment (EPT) is a method that combines electrochemical reactions and thermal effects, creating optimal conditions for phase transformations and modification of the metal surface layer. Thanks to the combination of intensive heating and rapid cooling, this process ensures the formation of a finely dispersed structure including high-strength phases. This significantly improves the mechanical properties of the material, such as hardness, wear resistance and resistance to fatigue loads. The application of thermocyclic regimes in EPT promotes the accumulation of structural changes, which is achieved through multiple phase transformations and regulation of temperature parameters [7].

The choice of thermocyclic treatment parameters, such as temperature, number of cycles, heating and cooling rates, allows the method to be adapted to the specific requirements of industrial production. This makes electrolyte-plasma treatment not only highly efficient but also energy-efficient, which is especially important for modern manufacturing processes. Moreover, the possibility of combining EPT with other treatment and modification methods opens new horizons for complex improvement of materials performance [8].

The purpose of this study is to investigate the effect of thermocyclic electrolytic-plasma treatment on the mechanical properties of U9 tool steel. The work is aimed at detailed analysis of changes in microstructure, hardness and strength characteristics of the material after treatment. The results obtained will make it

possible to evaluate the potential of this method to improve the reliability and durability of parts used in mechanical engineering and equipment manufacturing.

Materials and methods of research

The object of the study was U9 carbon tool steel. The choice of the research material is justified by the fact that this steel is widely used in mechanical engineering, power engineering and other industries, where such properties as strength, wear resistance, ability to maintain mechanical characteristics under high loads are important [9]. U9 carbon tool steel has high hardness, which makes it indispensable in the production of cutting and measuring tools, as well as elements of stamping systems. Knives, cutters, drills, calipers, files, punches and dies are made of this steel. Chemical composition of U9 tool steel according to GOST 1435-99 is presented in Table 1.

Table 1

Chemical composition of U9 tool steel

C	Si	Mn	Ni	S	P	Cr	Cu	V	Mo
0.85–0.94	0.17–0.33	0.17–0.33	until 0.25	until 0.028	until 0.03	until 0.2	until 0.25	–	–

Samples were prepared on a Metapol-2000P surface grinding machine with subsequent polishing using diamond pastes. At least 5 samples were used for each batch for reliability of measurement results.

The microstructure of the samples was revealed by chemical etching method using 4 % nitric acid solution (HNO_3) in ethyl alcohol. The microstructure of initial and treated steels was studied by optical microscopy on Olympus BX53P microscope in reflected light at light field and scanning electron microscopy (SEM) on "TESCAN VEGA 4" microscope at magnifications ×4000, ×10000. The imaging was carried out in the regimes of secondary and backscattered electrons.

To determine the hardness by depth of the samples we used a hardness micro-measurer Metolab 502 equipped with a four-sided diamond Vickers pyramid with a square base and angle $\alpha = 136°$ between opposite faces at the apex in strict compliance with the requirements of GOST 9450-76 for the Vickers method. The diamond indenter under the load $F = 1$N was pressed in perpendicularly and held under the load for 10 s. The diagonals of the indentation $d1$, $d2$ were measured.

The study of electro-discharge phenomena in the "metal-electrolyte" system. Tests were carried out to determine the values of hydrogen ion activity (pH), as well as the values of the electric potential of electrolytes, and the molar concentrations of electrolytes were calculated.

The electrolytes were prepared on the basis of soda ash (Na_2CO_3) diluted with water (H_2O), the equation reaction is presented in formula (1).

$$Na_2CO_3 + H_2O \rightarrow HCO_3^- + 2Na^+ + OH^- \quad (1)$$

As a result of a chemical reaction, a salt solution formed by a strong base and a weak acid gives an alkaline reaction (excess OH ions). The end products of the reaction are hydrogen carbonate (carbonic acid), sodium ions and hydroxide ions.

Two types of electrolyte based on sodium carbonate were prepared to study the properties, with a difference in its content in solution, namely for the first electrolyte the mass fraction was 15 % (No. 1), for the second 10 % (No. 2).

For preparation of electrolyte No. 1, 3 kg of Na_2CO_3 and 17 kg of distilled water were used. For electrolyte No. 2, 4 kg of Na_2CO_3 and 16 kg of distilled water.

The concentration of electrolytes was determined and experimental work was carried out to measure pH, specific conductivity and mass concentration of dissolved solute. Measurement of pH was carried out on laboratory ionometer I-160MI (production of Russia) according to GOST 8.120-99 "State verification scheme for pH measuring instruments". The instrument consists of primary measuring transducers — electrode system and temperature sensor (hereinafter — temperature sensor), secondary measuring transducer (hereinafter — transducer) and a set of accessories for measurements [10]. The general view of the transducer and its design elements are shown in Figure 1.

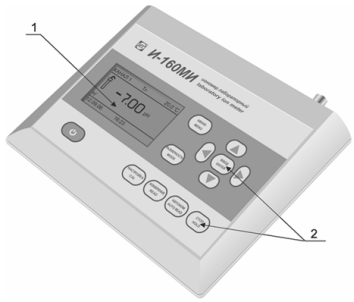

1 — Matrix display; *2* — Controls

Figure 1 Converter I-160MI

According to the methodology, before measurements, the electrodes are calibrated in buffer solutions with different pH values. No. 1 buffer solution pH = 1.65, No. 2 pH = 3.56, No. 3 pH = 9.18. Between each buffer solution and just before the measurements, the electrodes are cleaned from reagent residues with a stream of distilled water. Quality control of electrode cleaning from buffer solution residues is performed by measuring the pH value of distilled water. The pH value on the electrode surface should correspond to a neutral value (about 7) to exclude buffer solution residues. Once the electrodes have been calibrated, direct measurements are allowed. The electrodes are placed before the measuring part is immersed in the electrolyte for an average of 3 minutes. After that the display shows the finished values. Values were obtained for the initial electrolyte before TEPT, as well as after the 1st, 2nd, 3rd cycles. The results of pH, electrode potential measurements are presented in Table 2.

Calculations of molar concentration of electrolytes were carried out using formula 2. The data were obtained for 50 ml of electrolyte, which subsequently served as samples for the study of pH values, potentials.

$$C = \frac{m}{M \times V}, \tag{2}$$

where m — mass of sodium carbonate [g]; M — molar mass of sodium carbonate [g/mol]; V — volume of solution [l].

Thermocyclic electrolyte-plasma treatment of samples of steel U9 was carried out on the modernized unit in the Research Center “Surface Engineering and Tribology”. The modernized unit includes several key modules, which important elements are synchronization unit, microprocessor unit, power supply unit, power leads unit and control unit (Fig. 2 *A*). The synchronization unit is responsible for phasing and ensuring correct communication between the supply network and the thyristors. The microprocessor unit allows the thermal cycling parameters to be set, operating regimes to be set and the entire system to be automatically controlled. The power supply unit converts the input voltage to the necessary levels to support the operation of all other modules. The power output block provides high-power currents for processing steel samples, and the control block synchronizes the thyristors’ actions by switching them on and off at the right moments.

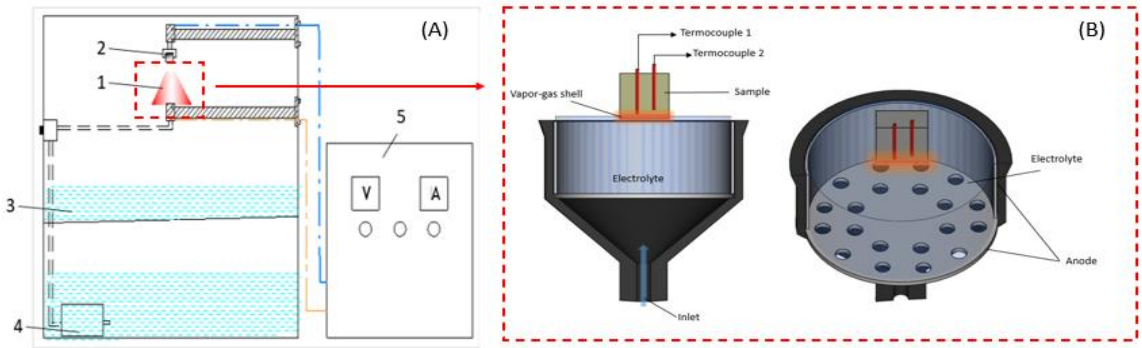

(*A*) Image of the unit for diffusion-electrolyte-plasma boriding:
1 — anode; *2* — sample; *3* — electrolyte bath; *4* — pump; *5* — power supply;
(*B*) Scheme of thermocouple placement in the surface layer of the sample

Figure 2. Schematic diagram of the general view of the EPT unit

During the experimental work, temperature measurements on the sample surface were carried out. For this purpose, thermocouples made by the method of natural thermal junction were used. Thermocouples were placed in two layers of the sample at a depth of 1.0 and 2.0 mm from the heated surface, which allowed recording temperature changes at different levels of the material (Fig. 2 *B*). When calculating the temperature at the sample surface, it was assumed that the entire heat flux propagates from the surface into the depth of the material. This assumption allows us to consider the thermal process unidirectional and take into account the influence of only those factors that are associated with energy transfer to the depth of the sample, without taking into account possible losses to radiation or convection. This approach simplifies the analysis and allows for a more accurate determination of the surface temperature [7, 8].

The essence of the thermocyclicelectrolyte-plasma treatment process is as follows. At low voltages (150 V), a classical electrochemical process is observed in an electrochemical cell containing an aqueous electrolyte solution. At higher voltages (300 V), an intensive electrode outgassing begins, leading to the formation of a near-electrode gas-liquid layer. As the voltage increases, the packing density of gas bubbles in the near-electrode gas-liquid layer increases, and the total cross-sectional area of electrolyte bridges between them decreases. As a result of Joule heat release, the electrolyte temperature in these bridges reaches the boiling point. During the transition from bubble boiling to film boiling, a thin (50–100 μm) vapor-gas shell (VGS) consisting of water vapor, activated OH^-, H^+ and Na^+ and CO_3^{2-} ions, which are part of the electrolyte, appears around the product immersed in the electrolyte. The electric field strength in VGS reaches 10^4–10^5 V/cm. At a temperature of about 100 °C, such a voltage can cause ionization of vapors, as well as emission of ions and electrons necessary to maintain a stationary electric discharge. And as a result, electrolyte plasma is formed [11]. Sodium carbonate (Na_2CO_3) solution was used as heating and cooling source.

A hardness tester “METOLAB 502” (GOST 6507-1-2007) was used to test the microhardness by the Vickers method. The indenter used for measurement was a diamond pyramid with an angle between two faces of 136°. The following regime was chosen to measure hardness by Vickers method: load 0.1 kg, load time 10 sec.

The study of surface microstructure and analysis of morphology of cross sections of coatings were carried out using scanning electron microscopy (SEM) on the equipment VEGA4 TESCAN in D. Serikbayev East Kazakhstan Technical University.

Results and discussion

The results of tests in the “metal-electrolyte” system are presented in Table 2.

Table 2

Results of electrochemical studies of TEPT electrolytes

	Cycle TEPT	1-Electrolyte composition: 15 % Na_2CO_3 + 85 % water	2-Electrolyte composition: 10 % Na_2CO_3 + 90 % water
Specific conductivity *s*, μSm/cm	1	83000	69000
	2	63000	43000
	3	51860	26400
Index, pH	1	10.759	10.675
	2	10.728	10.561
	3	10.778	10.620
Electrode potential, *E*°, mV	1	–223.6	–231.4
	2	–222.4	–227.7
	3	–223.6	–229.1
Molar concentration, *C*, mol/L	1	0.0047	0.0035
	2	0.0049	0.0036
	3	0.0043	0.0031

The initial pH values for electrolyte No. 1, No. 2 were 10.759 and 10.691, respectively. As can be seen from the data in Table 2, decrease in salt concentration and increase in water content decreases the pH value of electrolyte. The result of electrode potential measurement for the two electrolytes showed negative value, namely for electrolyte No. 1 –223.6 and for electrolyte No. 2 –231.4. This is due to the high concentration of OH^- ions in the electrolyte, which reduce the concentration of hydrogen ions and make the electric potential relative to the standard hydrogen electrode negative. As the pH value of the solution increases, the electrode

potential becomes more negative. This is an expected pattern because an increase in pH indicates a decrease in the concentration of H^+ ions, which shifts the equilibrium of the electrochemical reaction. According to the results of electrolyte concentration calculations, a slight change in molar concentrations is observed before and after several cycles [12–14].

Table 3 presents the results of electrolyte-plasma treatment experiments on U9 steel conducted in sodium carbonate (Na_2CO_3) solutions with 15 % and 10 % concentration. During the experiments, the effects of parameters such as voltage, current strength, heating duration and electrolyte concentration on steel surface temperature, current density and temperature changes of the electrolyte were studied. Using a 15 % Na_2CO_3 solution, the electrolyte temperature was 35–36 °C before heating and reached 39 °C after the third cycle. In the first cycle, at a voltage of 300 V, a current of 100 A and a heating time of 2 seconds, the steel surface temperature reached 374 °C at a current density of 33.3 A/cm². In subsequent cycles, despite short heating periods (300 V for 1–2 seconds), the surface temperature increased significantly, reaching 800 °C in the second cycle and 1000 °C in the third cycle. The intermediate voltage reduction to 150 V for 3 seconds helped to stabilize the process and to distribute the heat evenly, preventing overheating of the steel surface.

For the 10 % Na_2CO_3 solution, similar trends were observed, but with a lower heating intensity. The initial electrolyte temperature was slightly lower (34.9–36.7 °C) and the current density was 13.3 A/cm², which was about 2.5 times lower than that of the 15 % solution. The steel surface temperature reached 350 °C in the first cycle, 700 °C in the second cycle, and a maximum value of 1200 °C in the third cycle. Increasing the heating duration (up to 5 seconds at 300 V) combined with intermediate pauses at 150 V provided smoother surface heating. This makes the 10 % solution suitable for applications where a more gradual and delicate temperature rise is required without the risk of significant thermal stresses.

Table 3

Parameters of electrolyte-plasma treatment of U9 steel in Na_2CO_3 solutions with different concentrations

Steel	Electrolyte	*T*, °C	*U*, V	*t*, s	*I*, A	Cycle	*T*, °C Steel	*J*, A/cm^2
U9	10 % Na_2CO_3	before 36.7	300	5	40	1	350	13.3
		after 37.4	150	5	9			3
			300	4	40			13.3
			150	5	9			3
		before 34.9	300	5	40	2	700	13.3
		after 36.3	150	5	9			3
			300	4	40			13.3
			150	5	9			3
		before 35.6	300	5	40	3	1200	13.3
		after 37.3	150	5	9			3
			300	4	40			13.3
			150	5	9			3
	15 % Na_2CO_3	before 36	300	2	100	1	374	33.3
		after 36.6	150	3	60			20
			300	1	100			33.3
			150	3	60			20
		before 35	300	2	100	2	800	33.3
		after 36.3	150	3	60			20
			300	1	100			33.3
			150	3	60			20
		before 35	300	2	100	3	1000	33.3
		after 39	150	3	60			20
			300	1	100			33.3
			150	3	60			20

Figure 3 shows the results of studies that were conducted to investigate the effect of electrolyte-plasma treatment on the microstructure and mechanical properties of U9 steels. The linear decrease in hardness with depth is associated with the appearance of zonal structure after TEPT. The highest hardness was shown by the samples processed in the mode of 3 cycles for both electrolyte compositions. Also the smallest difference for 3 cycles showed the samples treated with TEPT using the first electrolyte composition (15 % Na_2CO_3). In

further studies the samples hardened in the first electrolyte composition were used. In the dissertation work the author Z.A. Satbaeva gives similar data on the dependence of microhardness on the depth of hardened layer for steel U10. In this work, the dependence of hardness decreases with deepening into the hardened material [15].

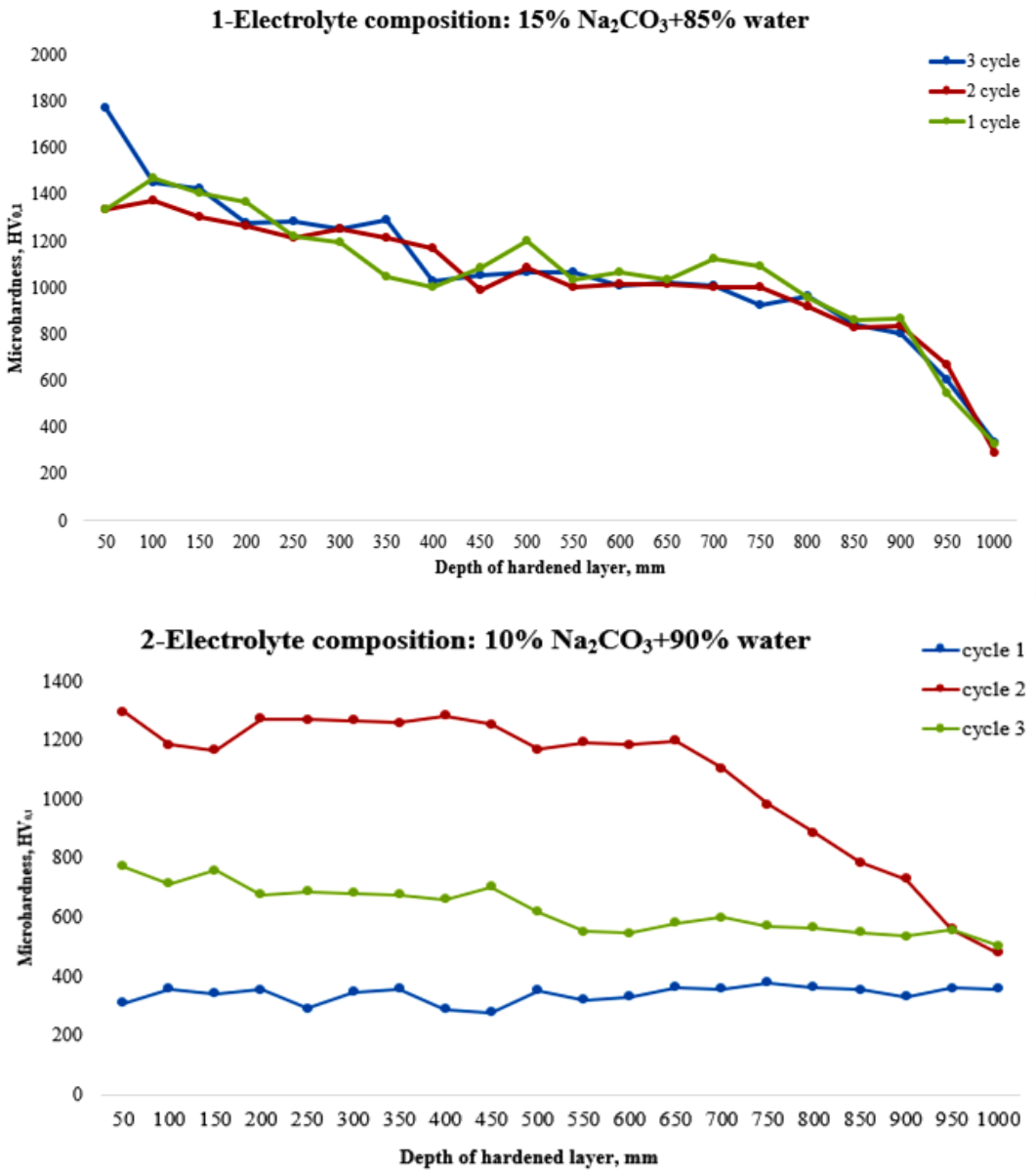

Figure 3. Dependence of microhardness of U9 steels on regimes of electrolyte-plasma treatment and electrolyte concentration

Figure 4 shows the results of electrolyte-plasma treatment of U9 steel in 10 % Na_2CO_3 solution at regime (cycle) No. 1. The microstructure of the material is clearly divided into three zones: hardened layer, transition layer and base metal. The hardened layer, located up to a depth of about 400 μm, shows a finely dispersed structure consisting of martensite and bainite, which provides a high hardness of the material at 1400–1600 $HV_{0.1}$. This layer is formed under the influence of intense heating and rapid cooling, resulting in phases with high strength. This structure provides a significant increase in the wear resistance of the surface, making it suitable for high mechanical stresses.

The transition layer, located at a depth of 400 μm to 700 μm, is characterized by a gradual change in the material structure. In this zone there is a decrease in hardness to the level of 800–1200 $HV_{0.1}$, which is associated with a decrease in thermal effects. Here, pre-eutectoid ferrite is isolated, which forms a mesh along grain boundaries, and the structure acquires a multigrain character. Slow cooling in this region favors the

preservation of fine phases, but the martensite content decreases, which leads to a decrease in strength properties [15, 16]. The transition layer plays an important role as a buffer zone, evenly distributing mechanical stresses between the hardened zone and the base metal, preventing abrupt changes in material properties.

In the base metal zone, deeper than 700 μm, the structure returns to the original structure. Here, an increase in ferrite content is noticeable both at grain boundaries and within them. Microhardness in this zone decreases significantly to 400–600 $HV_{0.1}$, indicating the recovery of properties characteristic of the base metal. This zone is practically not exposed to heat, and its properties correspond to the initial mechanical characteristics of the material. The microhardness graph clearly demonstrates a sharp decrease in hardness with increasing depth, starting from the hardened layer and moving to the base metal.

Thus, electrolyte-plasma treatment of U9 steel forms a high-strength hardened layer with a smooth transition to the transition zone and the base metal.

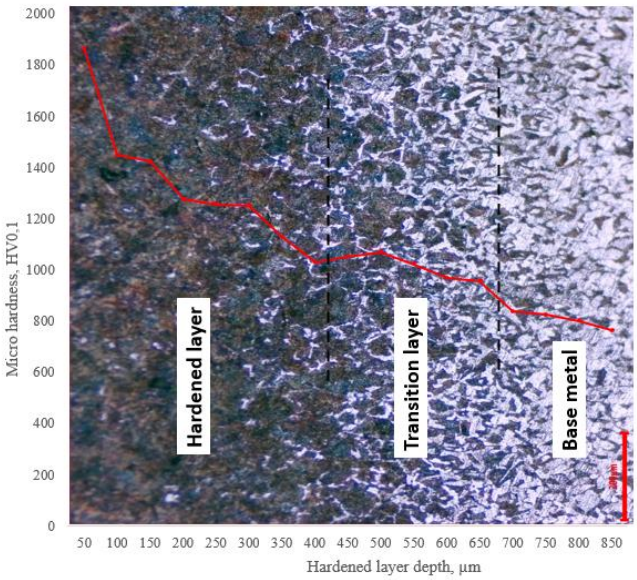

Figure 4. Microstructure and microhardness distribution of U9 steel after electrolyte-plasma treatment (regime No. 1, 15 % Na_2CO_3)

Figure 5 shows the microstructure of U9 steels after treatment with 15 % electrolyte, in three different regimes (No. 1, No. 2, No. 3), which allows us to draw conclusions about the influence of thermal conditions on the formation of structure and mechanical properties of materials. U9 steel, which has high carbon content, in regime No. 1 shows a microstructure mainly consisting of finely dispersed martensite, which confirms its quenched state and provides the highest hardness among all three regimes. In regime No. 2, the structure includes both martensite and bainite due to the milder cooling conditions. This results in intermediate properties between the quenched state and the slow cooling state. In regime No. 3, the microstructure of U9 steel is represented by ferrite and pearlite, which is characteristic of slow cooling. This leads to a significant decrease in hardness and return of the material to a state close to the initial.

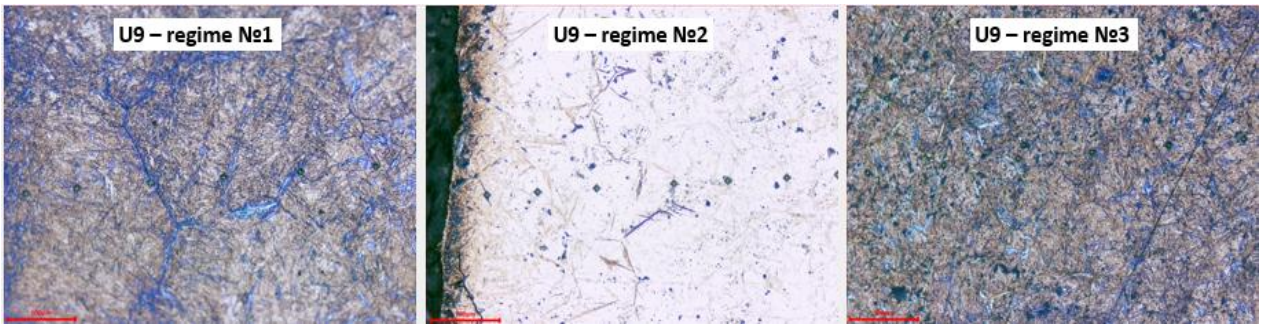

Figure 5. Cross-sectional microstructure of U9 steels after EPT in regimes No. 1, No. 2 and No. 3

To study in detail the structure of U9 steel after electrolyte-plasma treatment, the studies were carried out using scanning electron microscopy (SEM). The results of the analysis confirmed the presence of clearly defined three zones, each characterized by unique microstructure and mechanical properties (Fig. 6). The hardened layer, located at a depth of up to 400 μm, is formed under the influence of intense thermal heating and rapid cooling, resulting in the formation of finely dispersed phases such as martensite and bainite. This structure provides high hardness of the material, reaching 1400–1600 $HV_{0.1}$, which makes it extremely wear-resistant and suitable for high mechanical stresses. The micrographs obtained under magnification clearly show that the martensitic structure has a needle-like character, which confirms its high strength and stiffness. The transition layer, located at a depth of 400 μm to 700 μm, shows changes in the microstructure as it moves away from the hardened zone. In this region, a decrease in thermal stress is observed, leading to a decrease in martensite content and a gradual increase in the proportion of pre-eutectoid ferrite. Slow cooling in the transition zone favors the preservation of finely dispersed phases, but the overall strength of the material is lower here compared to the hardened layer. The transition layer plays a key role as a buffer zone, preventing abrupt changes in mechanical properties between the high-strength surface and the lower-strength base metal. The base metal deeper than 700 μm is virtually unaffected by heat during machining. Its structure reverts to the initial state characteristic of U9 steel and includes ferrite and pearlite. In micrographs, the base metal is characterized by the presence of large ferrite grains located both along the grain boundaries and inside the grains. The hardness in this zone is much lower, varying between 400–600 $HV_{0.1}$, which corresponds to the initial mechanical characteristics of the material. This region retains the ductility and toughness characteristic of the initial state of the steel and plays an important role in preventing brittleness of the structure as a whole. Thus, electrolyte-plasma treatment allows the creation of a functionally graded structure consisting of three zones with different mechanical properties: a high-strength hardened layer, a transition layer and the base metal. This distribution of properties ensures high operational reliability of the material, improves its wear resistance and resistance to mechanical loads.

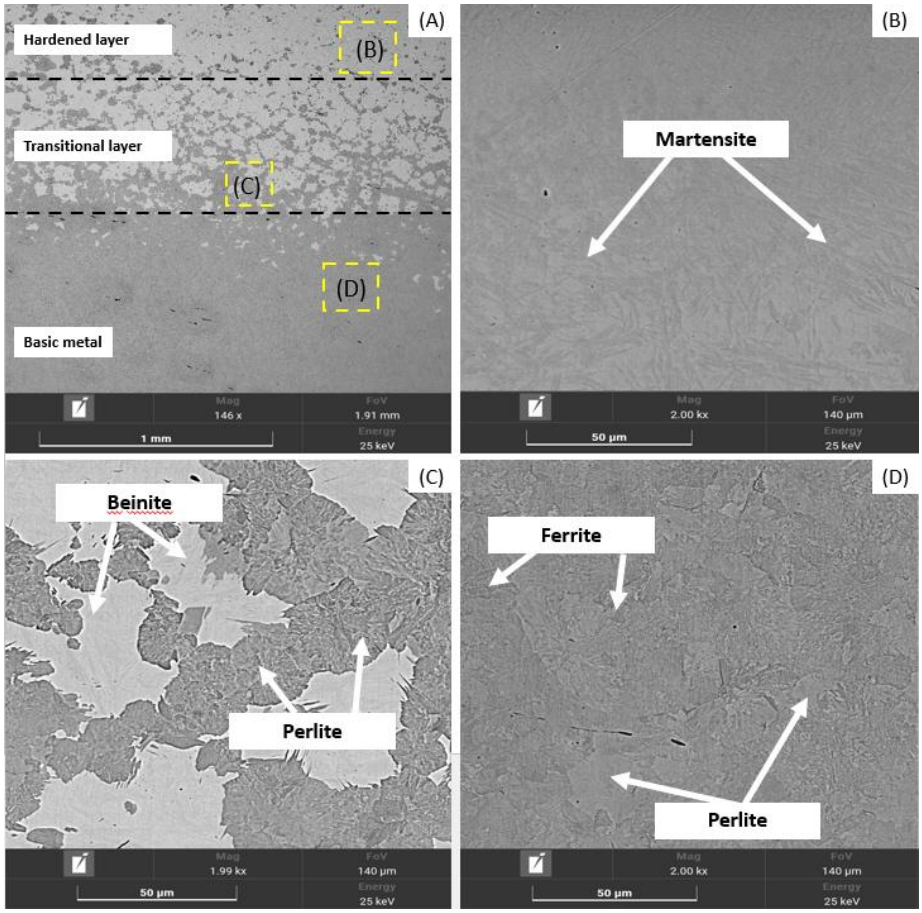

Figure 6. Microstructure of different zones of U9 steel after electrolytic-plasma treatment (regime No. 1)

Conclusion

Thus, according to the results obtained in this article, the following main findings and conclusions were made:

– the electrode potential becomes more negative as the pH value of the solution increases. According to the results of electrolyte concentration calculations, a slight change in molar concentrations is observed before and after several cycles.

– for the 10 % Na_2CO_3 solution, a decrease in heating intensity was observed. The initial electrolyte temperature was slightly lower (34.9–36.7 °C) and the current density was 13.3 A/cm², which is about 2.5 times lower than that of the 15 % solution. This makes the 10 % solution suitable for applications where a more gradual and delicate temperature rise is required without risks of significant thermal stresses.

– electrolytic-plasma treatment of U9 steel in 10 % Na_2CO_3 solution forms a hardened layer (up to 400 μm) with finely dispersed martensite and bainite structure and hardness of 1400–1600 $HV_{0.1}$, providing high wear resistance. The transition layer (400–700 μm) serves as a buffer, reducing hardness to 800–1200 $HV_{0.1}$ and evenly distributing stresses. In the base metal zone (deeper than 700 μm), the structure returns to its original structure with a hardness of 400–600 $HV_{0.1}$. The method creates a strong surface layer and a smooth transition to the basic material properties.

Acknowledgments

This research is funded by the Science Committee of the Ministry of Science and Higher Education of the Republic of Kazakhstan (Grant No. BR24992879).

References

1 Kusmanov S. Increasing Hardness and Wear Resistance of Austenitic Stainless Steel Surface by Anodic Plasma Electrolytic Treatment / T. Mukhacheva, I. Tambovskiy, A. Naumov, R. Belov, E. Sokova, I. Kusmanova // Metals. — 2023. — Vol. 13. — P. 872.

2 Belkin P.N. Plasma Electrolytic Saturation of Steels with Nitrogen and Carbon / P.N. Belkin // Critical Reviews in Solid State and Materials Sciences. — 2011. — Vol. 36(3). — P. 174–190.

3 Aliofkhazraei M. Nano-Fabrication by Cathodic Plasma Electrolysis / A.R. Aghdam, P. Gupta // Critical Reviews in Solid State and Materials Sciences. — 2011. — Vol. 36(3). — P. 174–190.

4 Meletis E.I. Electrolytic plasma processing for Cleaning and Metal coating of Steel Surface / X. Nie, F.L. Wang, J.C. Jiang // Surface and Coatings Technology. — 2002. — Vol. 150. — P. 246–256.

5 Kusmanov S.A. Anode plasma electrolytic nitrohardening of medium carbon steel / A.A. Smirnov, Yu.V. Kusmanova, P.N. Belkin // Surface and Coatings Technology. — 2015. — Vol. 269. — P. 308–313.

6 Смирнов А.А. Повышение коррозионной стойкости и износостойкости стали 45 с помощью анодного электролитно-плазменного азотирования / А.А. Смирнов, С.А. Силкин, П.Н. Белкин, И.Г. Дьяков, В.С. Севостьянова, С.А. Кусманов // Изв. вузов. Химия и хим. технолология. — 2017. — Т. 60. — Вып. 1. — С. 81-86.

7 Dautbekov M.K. A Technology for Making Detonation Coatings on Power Equipment Parts Made of Grade 12Kh1MF Steel / B.K. Rakhadilov, L.G. Zhurerova, D.N. Kakimzhanov, S.L. Elistratov, T.A. Segeda // Thermal Engineering. — 2022. — Vol. 69(12). — P. 989–995.

8 Baizhan D. Investigation of Changes in the Structural-Phase State and the Efficiency of Hardening of 30CrMnSiA Steel by the Method of Electrolytic Plasma Thermocyclic Surface Treatment / D. Baizhan, B. Rakhadilov, L. Zhurerova, Y. Tyurin, Z. Sagdoldina, M. Adilkanova, R. Kozhanova // Coatings. — 2022. — Vol. 12(11). — P. 1996.

9 Rakhadilov B.K. Study of the VAC of the EPCTT process with varying electrode parameters / B.K. Rakhadilov, N.E. Berdimuratov, L.G. Zhurerova, L.B. Bayatanova, Sh.R. Kurbanbekov, Z.A. Satbayeva // Bulletin of the University of Karaganda-Physics. — 2023. — Vol. 3(111). — P. 136–142. DOI: https://doi.org/10.31489/2023PH3/136-142.

10 Zhou L. Additive Manufacturing: A Comprehensive Review / L. Zhou, J. Miller, J. Vezza, M. Mayster, M. Raffay, Q. Justice, Z. Al Tamimi, G. Hansotte, L.D. Sunkara, J. Bernat // Sensors. — 2024. — Vol. 24(6). — P. 2668. DOI: https://doi.org/10.3390/s24092668.

11 Belkin P.N. Plasma electrolytic saturation of steels with nitrogen and carbon / P.N. Belkin, A.L. Yerokhin, S.A. Kusmanov // Surf. Coat. Technol. — 2016. — Vol. 307. — P. 1194–1218.

12 Kusmanov S.A. Modification of steel surface by plasma electrolytic saturation with nitrogen and carbon / S.A. Kusmanov, Y.V. Kusmanova, A.A. Smirnov, P.N. Belkin // Mater. Chem. Phys. — 2016. — Vol. 175. — P. 164–171.

13 Zhan S. Cathodic Discharge Plasma in Electrochemical Jet Machining: Phenomena / S. Zhan, Z. Lyu, B. Dong, W. Liu, Y. Zhao // Mechanism and Characteristics. Int. J. Mach. Tools Manuf. — 2023. — Vol. 187. — P. 104015. DOI: https://doi.org/10.1016/j.ijmachtools.2023.104015.

14 Gupta P. Plasma Formation and Material Removal Characteristics in Microwave-Metal Discharge-Based Machining of AISI 304 Stainless Steel. J. Manuf / P. Gupta, A.K. Sharma, I. Singh. // Process. — 2024. — Vol. 124. — P. 1159–1179. DOI: https://doi.org/10.1016/j.jmapro.2024.06.069.

15 Сатбаева З.А. Структурообразование в легированных сталях при электролитно плазменном поверхностном упрочнении: дис. ... д-ра философии (PhD) : 6D060400 — Физика / З.А. Сатбаева. — Усть-Каменогорск, 2022. — 119 с.

16 Tang W. Experimental Investigation of Discharge Phenomena in Electrochemical Discharge Machining Process / W. Tang, Y. Zhu, X. Kang, C. Mao // Micromachines. — 2023. — Vol. 14 — P. 367. DOI: https://doi.org/10.3390/mi14020367.

17 Asmael M. A Review on Recent Achievements and Challenges in Electrochemical Machining of Tungsten Carbide / M. Asmael, A. Memarzadeh // Archives of Advanced Engineering Science. — 2023. — Vol. 2(1). — P. 1–23. DOI: https://doi.org/10.47852/bonviewaaes3202915.

Л.Г. Сулюбаева, Д.Б. Буйткенов, Д.Р. Байжан,
Н.Е. Бердімуратов, Н.С. Райсов, А.Ж. Жумабеков

У9 құралдық болаттың механикалық қасиеттеріне термоциклдік электролитті-плазмалық өңдеудің әсері

Мақалада термоциклдік электролитті-плазмалық өңдеудің (ЭПӨ) У9 көміртекті құралдық болаттың механикалық қасиеттеріне әсері қарастырылған. У9 болаты ағаш өңдеу құралдары, слесарлық-монтаждық аспаптар, қарапайым пішінді калибрлер және дәлдік кластарын төмендетуде жиектерін қыздырмайтын жағдайларда жұмыс істейтін құралдарды өндіру үшін кеңінен қолданылады. Осы жұмыста механикалық қасиеттерді жақсарту әдісі ретінде термоциклдік электролитті-плазмалық өңдеу пайдаланылды. Бұл әдіс электрхимиялық реакциялармен қарқынды термиялық әсерді біріктіріп, жақсартылған сипаттамалары бар беттік қабаттардың пайда болуына мүмкіндік береді. Өңдеу нәтижесінде У9 болаты микроқұрылымның үш аймаққа анық бөлінуін көрсетеді: берiктелген қабат, өтпелі қабат және негізгі металл. 400 мкм тереңдікте орналасқан беріктендірілген қабат ұсақдисперсті құрылыммен сипатталады. Ол мартенсит пен бейниттен тұрады, қаттылығы жоғары (1400–1600 $HV_{0{\cdot}1}$). Бұл қабат жоғары тозуға төзімділікті және механикалық жүктемелерге беріктікті қамтамасыз етеді. 700 мкм тереңдікте орналасқан өтпелі қабат кернеулерді біркелкі тарататын буферлік аймақ қызметін атқарады. Ол қаттылықтың бірте-бірте төмендеуімен (800–1200 $HV_{0{\cdot}1}$) және мартенсит құрамының төмендеуіне байланысты құрылымның өзгеруімен сипатталады. Тереңдігі 700 мкм-ден асатын негізгі металл 400–600 $HV_{0{\cdot}1}$ қаттылығымен өзінің бастапқы құрылымын сақтайды, бұл оның икемділігі мен ұзақ мерзімділігін қамтамасыз етеді. Алынған нәтижелер ЭПӨ термоциклдік функционалды градиент құрылымын жасай отырып, У9 болатының эксплуатациялық қасиеттерін айтарлықтай жақсартатынын көрсетеді. Бұл технология энергия тиімділігі тұрғысынан үнемді және машина жасауда және материалдардың жоғары механикалық сипаттамаларын қажет ететін басқа да салаларда кеңінен қолданылуы мүмкін.

Кілт сөздер: термоөңдеу, термоциклдік электролитті-плазмалық өңдеу, электр разрядтық құбылыстар, У9 құралдық көміртекті болаты, микроқұрылым

Л.Г. Сулюбаева, Д.Б. Буйткенов, Д.Р. Байжан,
Н.Е. Бердимуратов, Н.С. Райсов, А.Ж. Жумабеков

Влияние термоциклической электролитно-плазменной обработки на механические свойства инструментальной стали У9

В статье исследуется влияние термоциклической электролитно-плазменной обработки (ЭПО) на механические свойства инструментальной углеродистой стали У9. Сталь У9 широко используется для изготовления инструментов, работающих в условиях, не вызывающих разогрева кромки, таких как инструмент для обработки дерева, слесарно-монтажный инструмент, калибры простой формы и пониженных классов точности. В данной работе методом улучшения механических свойств используется термоциклическая электролитно-плазменная обработка. Этот метод объединяет электрохимические реакции и интенсивное термическое воздействие, что позволяет формировать поверхностные слои с улучшенными характеристиками. В результате обработки сталь У9 демонстрирует чёткое разделение микроструктуры на три зоны: упрочнённый слой, переходный слой и основной металл. Упрочнённый слой, расположенный до глубины 400 мкм, характеризуется мелкодисперсной структурой. Она состоит из мартенсита и бейнита, с высокой твёрдостью (1400–1600 $HV_{0{\cdot}1}$). Этот слой обеспечивает превосходную износостойкость и устойчивость к механическим нагрузкам. Переходный слой, расположенный до глубины 700 мкм, служит буферной зоной, равномерно распределяя напряжения. Он характеризуется постепенным снижением твёрдости (800–1200 $HV_{0{\cdot}1}$) и изменением структуры за счёт

уменьшения содержания мартенсита. Основной металл, глубже 700 мкм, сохраняет исходную структуру с твёрдостью 400–600 $HV_{0.1}$, что обеспечивает его пластичность и долговечность. Полученные результаты показывают, что термоциклическая ЭПО значительно улучшает эксплуатационные свойства стали У9, создавая функционально градиентную структуру. Данная технология эффективна с точки зрения энергоэкономичности и может найти широкое применение в машиностроении и других отраслях, требующих высоких механических характеристик материалов.

Ключевые слова: термообработка, термоциклическая электролитно-плазменная обработка, электроразрядные явления, инструментальная углеродистая сталь У9, микроструктура

References

1 Kusmanov, S., Mukhacheva, T., Tambovskiy, I., Naumov, A., Belov, R., Sokova, E., & Kusmanova, I. (2023). Increasing Hardness and Wear Resistance of Austenitic Stainless-Steel Surface by Anodic Plasma Electrolytic Treatment. *Metals*, *13,* 872.

2 Belkin, P.N. (2011). Plasma Electrolytic Saturation of Steels with Nitrogen and Carbon. *Critical Reviews in Solid State and Materials Sciences, 36*(3), 174–190.

3 Aliofkhazraei, M., Aghdam, A.R., & Gupta, P. (2011). Nanofabrication by Cathodic Plasma Electrolysis. *Critical Reviews in Solid State and Materials Sciences*, *36*(3), 174–190.

4 Meletis, E.I., Nie, X., Wang, F.L., & Jiang, J.C. (2002). Electrolytic plasma processing for Cleaning and Metal coating of Steel Surface. *Surface and Coatings Technology*, *150,* 246–256.

5 Kusmanov, S.A., Smirnov, A.A., Kusmanova, Yu.V., & Belkin, P.N. (2015). Anode plasma electrolytic nitrohardening of medium carbon steel. *Surface and Coatings Technology*, *269,* 308–313.

6 Smirnov, A.A., Silkin, S.A., Belkin P.N., Dyakov I.G., Sevostyanova V.S., & Kusmanov S.A. & (2017). Povyshenie korrozionnoi stoikosti i iznosostoikosti stali 45 s pomoshchiiu anodnogo elektrolitno-plazmennogo azotirovaniia [Improvement of corrosion and wear resistance of 45 steel with anode plasma electrolyte nitriding]. *Izvestiia Vysshikh Uchebnykh Zavedenii. Seriia "Khimiia i Khimicheskaia Tekhnologiia" — News of Higher Educational Institutions. The series "Chemistry and Chemical Technology", Vol. 60(1), Issue1,* 81–86 [in Russian].

7 Dautbekov, M.K., Rakhadilov, B.K., Zhurerova, L.G., Kakimzhanov, D.N., Elistratov, S.L., & Segeda, T.A. (2022). A Technology for Making Detonation Coatings on Power Equipment Parts Made of Grade 12Kh1MF Steel. *Thermal Engineering*, *69*(12), 989–995.

8 Baizhan, D., Rakhadilov, B., Zhurerova, L., Tyurin, Y., Sagdoldina, Z., Adilkanova, M., & Kozhanova, R. (2022). Investigation of Changes in the Structural-Phase State and the Efficiency of Hardening of 30CrMnSiA Steel by the Method of Electrolytic Plasma Thermocyclic Surface Treatment. *Coatings*, *12*(11), 1996.

9 Rakhadilov, B.K., Berdimuratov, N.E., Zhurerova, L.G., Bayatanova, L.B., Kurbanbekov, Sh.R., & Satbayeva, Z.A. (2023). Study of the VAC of the EPCTT process with varying electrode parameters. *Bulletin of the University of Karaganda-Physics*, *3*(111), 136–142. DOI: https://doi.org/10.31489/2023PH3/136-142.

10 Zhou, L., Miller, J., Vezza, J., Mayster, M., Raffay, M., Justice, Q., Al Tamimi, Z., Hansotte, G., Sunkara, L.D., & Bernat, J. (2024). Additive Manufacturing: A Comprehensive Review. *Sensors*, *24*(6), 2668. DOI: https://doi.org/10.3390/s24092668.

11 Belkin, P.N., Yerokhin, A.L., & Kusmanov, S.A. (2016). Plasma electrolytic saturation of steels with nitrogen and carbon. *Surf. Coat. Technol*, *307*, 1194–1218.

12 Kusmanov, S.A., Kusmanova, Y.V., Smirnov, A.A., & Belkin, P.N. (2016). Modification of steel surface by plasma electrolytic saturation with nitrogen and carbon. *Mater. Chem. Phys*, *175*, 164–171.

13 Zhan, S., Lyu, Z., Dong, B., Liu, W., & Zhao, Y. (2023). Cathodic Discharge Plasma in Electrochemical Jet Machining: Phenomena Mechanism and Characteristics. *Int. J. Mach. Tools Manuf*, *187,* 104015. DOI: https://doi.org/10.1016/j.ijmachtools.2023.104015.

14 Gupta, P., Manuf, J., Sharma, A.K., & Singh, I. (2024). Plasma Formation and Material Removal Characteristics in Microwave-Metal Discharge-Based Machining of AISI 304 Stainless Steel. *Process*, *124,* 1159–1179. DOI: https://doi.org/10.1016/j.jmapro.2024.06.069.

15 Satbaeva, Z.A. (2022). Strukturoobrazovanie v legirovannykh staliakh pri elektrolitno plazmennom poverkhnostnom uprochnenii [Structure formation in alloy steels during electrolytic plasma surface hardening]. *Doctor's thesis.* Ust-Kamenogorsk [in Russian].

16 Tang, W., Zhu, Y., Kang, X., & Mao, C. (2023). Experimental Investigation of Discharge Phenomena in Electrochemical Discharge Machining Process. *Micromachines*, 14, 367. DOI: https://doi.org/10.3390/mi14020367.

17 Asmael, M., & Memarzadeh, A. (2023). A Review on Recent Achievements and Challenges in Electrochemical Machining of Tungsten Carbide. *Archives of Advanced Engineering Science*, *2*(1), 1–23. DOI: https://doi.org/10.47852/bonviewaaes3202915.

Information about the authors

Laila, Sulyubayeva — PhD, Associate Professor, Senior Researcher of Scientific Research Center "Surface Engineering and Tribology", S. Amanzholov East Kazakhstan University, Ust-Kamenogorsk, Kazakhstan; e-mail: lsulyubayeva@gmail.com; ORCID ID: https://orcid.org/0000-0002-1924-1459

Dastan, Buitkenov — PhD, Leading Researcher of Scientific Research Center "Surface Engineering and Tribology", S. Amanzholov East Kazakhstan University, Ust-Kamenogorsk, Kazakhstan; e-mail: buitkenov@gmail.com; ORCID ID: https://orcid.org/0000-0002-0239-5849

Baizhan, Daryn — Senior Researcher of Scientific Research Center "Surface Engineering and Tribology", S. Amanzholov East Kazakhstan University, Ust-Kamenogorsk, Kazakhstan, 3rd year PhD of Shakarim University, Semey, Kazakhstan; e-mail: daryn.baizhan1@gmail.com, ORCID: https://orcid.org/0000-0002-9105-3129

Berdimuratov, Nurbol — Leading Researcher of Scientific Research Center "Surface Engineering and Tribology", S. Amanzholov East Kazakhstan University, Ust-Kamenogorsk, Kazakhstan; e-mail: nurbol.ber@gmail.com; ORCID ID: https://orcid.org/0009-0000-6880-6439

Nurmahanbet, Raisov (*corresponding author*) — Engineer of Scientific Research Center "Surface Engineering and Tribology", S. Amanzholov East Kazakhstan University, Ust-Kamenogorsk, Kazakhstan; e-mail: nurmakhanberraisov@gmail.com; ORCID ID: https://orcid.org/0009-0007-1698-957X

Almar, Zhumabekov — Doctor PhD of Physics, Associate Professor, Faculty Computer Science, Toraigyrov University, Pavlodar, Kazakhstan; e-mail: almar89-89@mail.ru; ORCID: https://orcid.org/0000-0003-2360-3747